CHEMICAL REACTIONS AT PHASE INTERFACES OF SLAG/INCLUSIONS AND STEEL/REFRACTORIES

Jung-Hwan Son, Sang-Chae Park, Jin-Hong Park, Sung-Mo Jung, Gaye & Hae-Geon Lee
POSTECH, Korea

In-Ho Jung
McGill University, Canada

ABSTRACT

Chemical reactions at the interface of different phases in the steel refining stage have been studied. Formation of intermediate phases at the reaction interface was examined at different conditions including inclusions dissolving into slag and reaction of glaze at the ladle refractory surface with molten steel. When inclusions dissolve into slag, three distinct dissolution patterns were identified, namely, monotonous dissolution without forming an intermediate phase, dissolution with forming intermediate phase(s) attached at the surface of inclusion, and dissolution with forming intermediate phase(s), but at some distance from the interface. The intermediate phases were critically identified and successfully explained with thermodynamic analysis. It was found that the dissolution rate was vastly different depending on the type of intermediate phase and its formation pattern. The dissolution rate was extremely slow when a spinel like $MgAl_2O_4$ and dicalcium silicate(Ca_2SiO_4) form as the interface.

Reaction of CaO-MgO-Al_2O_3-SiO_2 ladle slag glazed on high alumina refractory with Al-deoxidized molten steel was investigated with focus on the variation of microstructure and chemistry of the glazed refractory. Thermodynamic analysis was carried out simultaneously in order to understand the complex chemical reactions. During the reaction of the glazed refractory and molten steel, two chemical reactions were observed: chemical reaction between glaze and molten steel, and chemical reaction between glaze and original refractory. By the chemical reaction of the glazed refractory and molten steel, SiO_2 of glaze was reduced to [Si] by [Al] in molten steel. The glaze layer was changed gradually from the liquid CaO-MgO-Al_2O_3-SiO_2 phase with small amount of embedded spinel particles to the liquid CaO-MgO-Al_2O_3 phase with embedded spinel and $CaAl_4O_7$ particles. Severe erosion was observed in the porous spinel area of refractory. Spinel inclusion was found as a major inclusion originated from the glazed refractory. The erosion mechanism of the glazed refractory was proposed in the present study.

INTRODUCTION

Ladle glaze can be a source of non-metallic inclusions in the steel melt, which forms during the teeming of a ladle. Due to high temperature the ladle glaze may interact chemically with the ladle refractories. When the next heat is poured into the ladle, the solid glaze will melt again or react with liquid steel. In this way, exogenous inclusions can be generated from the ladle glaze.

Beskow et al. [1] studied the formation of ladle glaze and its impact on the generation of non-metallic inclusions in practical ladle treatment. Ladle lining (refractories) in their study was magnesia (carbon bearing MgO lining) refractories. Riaz et al. [2] and Hassall et al. [3] also performed similar studies at plant ladle treatment with magnesia refractories. The main concern of the most of the previous studies for ladle glaze was identification of inclusions and number of inclusions as the function of ladle age in a magnesia-lined ladle. In the present study fundamental research on the ladle glaze of a high alumina refractory lining was undertaken with emphasis on the formation of ladle glaze and its reaction with liquid steel containing Al and/or Ca.

Inclusions may be removed from the molten steel by floating up to the top slag phase in the ladle. In order to enhance steel cleanliness, the subjects of dissolution mechanisms and dissolution rates of non-metallic inclusions in molten slag and mold fluxes have been widely studied using various techniques, i.e. the rotating rod method and cylinder dipping method. Bygden et al. [4] and Zhang et al. [5] investigated the dissolution of MgO in the $CaO-FeO-SiO_2$ and $CaO-FeO-CaF_2-SiO_2$ slag, respectively. Yu et al. [6] studied the dissolution of Al_2O_3 in mold fluxes and Taira et al. [7] used the similar approach for Al_2O_3 dissolution in the $CaO-Al_2O_3-SiO_2$ slag. However, most of the previous studies were mainly concerned with refractory erosion, thus the applicability of these results to the kinetics of inclusion dissolution may be limited especially because the experiments were carried out with strong rotational speed of oxides (forced convection condition). The Confocal Scanning Laser Microscope (CSLM) has recently been applied to the in-situ observation of dissolution behaviors of inclusions in various molten slags. Use of CSLM has enabled to carry out more fundamental research on the dissolution mechanisms of inclusions. In the present study the dissolution behavior of MgO and $MgAl_2O_4$ particles in various $CaO-Al_2O_3-SiO_2-MgO$ slag at different temperatures were investigated using the confocal scanning laser microscope (CSLM). The direct dissolution rates of MgO and $MgAl_2O_4$ particles were measured, and the formation of continuous and discontinuous ring-like structures during the indirect dissolution of MgO particles was identified.

This presentation is the combined summary of several journal papers to be published by the authors [8, 9, 10].

EXPERIMENTAL

As-received refractory was cut to pieces in bar shape (10 mm x 30 mm x 100 mm) and dipped into liquid slag in order to prepare the glazed refractory specimen. Then, the specimen was dipped into Al-deoxidized or Al-deoxidized and Ca-treated molten steel. Table 1 shows the chemical compositions of as-received refractory and slag used in the present study. Details of the procedure can be found elsewhere [8, 9].

Table 1: Chemical compositions of as-received refractory, molten slag, initial liquid glaze and initial steel (wt%)

	CaO	MgO	Al_2O_3	SiO_2
As-received refractory	2.4	8.6	88.2	0.8
Molten slag	50.0	7.0	33.0	10.0

Initial liquid glaze	35.8	6.5	51.1	6.6
Initial Steel (total)	0.0012C-0.038Al-0.008Si-0.068Mn-0.009S-0.0087O			

The glazed refractory was dipped into the molten steel and then pulled out for furnace cooling at cooling rate. The effect of Ca-treatment of Al-deoxidized steel on the steel/refractory reaction was by adding Ca in the form of Ca-Si immediately after the dipping of a glazed refractory into Al-deoxidized molten steel.

The Confocal Scanning Laser Microscope (CSLM) equipped with a gold image furnace was employed to observe dissolution of inclusions in transparent and semi-transparent slags at high temperature. The apparatus was well explained in the previous study [11]. The compositions of the slag determined by the EPMA-WDS method were listed in Table 2 as (Liquidus and viscosity of each slag system were calculated using FactSage® and ViscFact® softwares, respectively).

Table 2: Experimental compositions of the $CaO-Al_2O_3-SiO_2-MgO$ slags used in the present study. (Liquidus and viscosity of each slag system were calculated using FactSage® and ViscFact®)

Slags	Slag composition (wt %)				CaO/SiO$_2$	Liquidus (°C)	Viscosity (poise)		
	CaO	SiO$_2$	MgO	Al$_2$O$_3$			1450°C	1500°C	1550°C
A	36.2	34.0	9.9	19.9	1.06	1424	8.52	6.46	4.96
B	30.2	40.1	9.9	19.8	0.75	1330	10.24	7.79	6.01
C	22.7	42.8	14.6	19.9	0.53	1373	10.06	7.77	6.06
D	9.8	45.0	25.1	20.1	0.22	1436	8.08	6.39	5.08
B-1	30.1	40.3	19.8	9.8	0.75	1370	4.47	3.46	2.71
B-2	31.8	42.9	15.4	9.9	0.74	1348	4.56	3.48	2.69
B-3	34.3	45.8	10.1	9.8	0.75	1331	6.02	4.51	3.42

Using a gold image furnace with a halogen lamp, the slag contained in the Pt crucible was heated to the predetermined expreimental temperature. More details of the experimental procedure can be found elsewhere [10].

RESULTS AND DISCUSSION

Steel/Refractory Interactions

As the typical contact time of ladle refractory with slag during teeming was estimated to be about 2 minutes, the dipping time of refractory into molten slag was determined to be 2 minutes in the present study. The thickness of the glazed layer was estimated to be about 150 ~ 200 μm as seen in Figure 1. Since molten slag contains much higher CaO compared with the original refractory, the Ca mapping identified the glazed layer and showed that the molten slag penetrated into the porous matrix of spinel phase. The close analysis of the glaze layer (A in Figure 1) showed that the glaze is composed of non-crystalline oxide and small amount of spinel particles. The composition of the liquid phase is almost homogeneously 39CaO-50Al$_2$O$_3$-7SiO$_2$-5MgO in mass%. The spinel particle size in the glaze layer widely ranged from sub-μm to 10 μm. Several different kinds of Ca-Al-O oxide phases ($CaAl_{12}O_{19}$, $CaAl_4O_7$ and $CaAl_2O_4$) were observed around a large and dense corundum particle when compared with solely $CaAl_{12}O_{19}$ phase in the case of the as-received refractory materials. As can be seen in the Ca mapping in Figure 1, this porous matrix was partially penetrated by the molten slag containing high CaO (54 mass%).
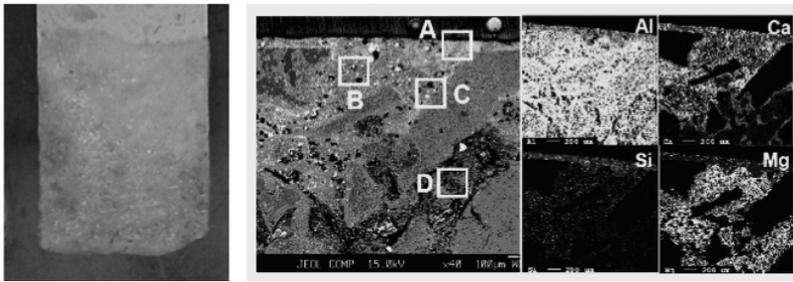
Figure 1: Photo image and microstructure and EPMA mapping images of the glazed
refractory after 2 min in contact with molten slag at 1600°C

The phase composition of the liquid glaze is quite different from the original slag. This means that the glaze is not an original slag but the reaction product of the molten slag and refractory in spite of such a short contact time as 2 minutes. Beskow *et al.* [1] studied the formation of ladle glaze on a magnesia lining in contact with $CaO-MgO-Al_2O_3-SiO_2$ ladle slag. They found that the glaze layer was composed of liquid $CaO-MgO-Al_2O_3-SiO_2$ phase and MgO island particles and that the slag penetrated into the porous area of the refractory during the glaze formation.

The EPMA mapping images of the glazed refractories are shown in Figure 2. The mapping images of Ca and Si clearly show the glazed layer and the penetration of liquid glaze into refractory materials. Therefore, the distributions of Ca and Si can give the clue for the reaction mechanism of the glazed refractory with molten steel. With reaction time, SiO_2 can diffuse into the porous matrix from the glaze layer like CaO. However, the SiO_2 concentration of the glaze layer became diluted in 5 minutes. In addition, no SiO_2 was detected up to a certain depth of the refractory in 10 minutes.

To investigate inclusions formed in the system, more than 20 inclusions were randomly selected for each sample. In general, Al_2O_3 inclusion was abundant in the early stage of the reaction, but its population decreased with reaction time. On the other hand, the population of spinel inclusions increased with time. The complex (Spinel + Al_2O_3) inclusions were also observed. The typical inclusions observed in the Al-deoxidized molten steel during the reaction with the glazed refractory at 1600°C are shown in Figure 3. In the beginning of the reaction, Al_2O_3 inclusion and its agglomerate (Figure 3a and 3c) were abundant. The shape of Al_2O_3 inclusion was irregular. The population of Al_2O_3 inclusions decreased with reaction time, and it almost disappeared after 15 minutes. Spinel inclusions began to be observed from 1 minute, and its population increased with reaction time. No spinel agglomerate was found. After 30 minutes, all inclusions were spinel inclusions.
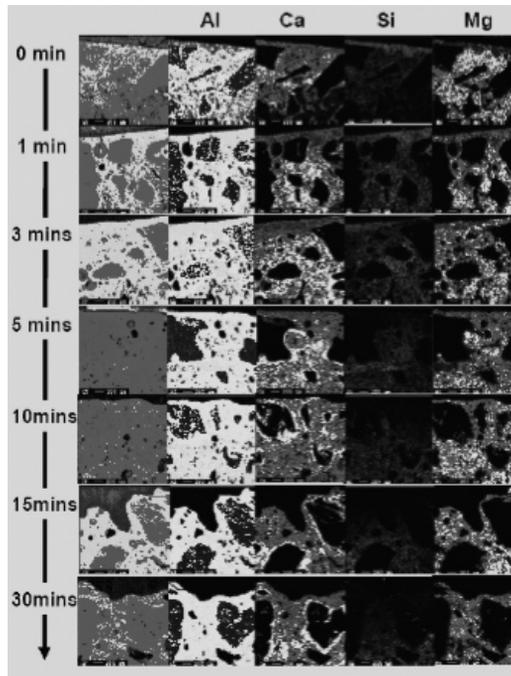
Figure 2: EPMA mapping images of the glazed refractories
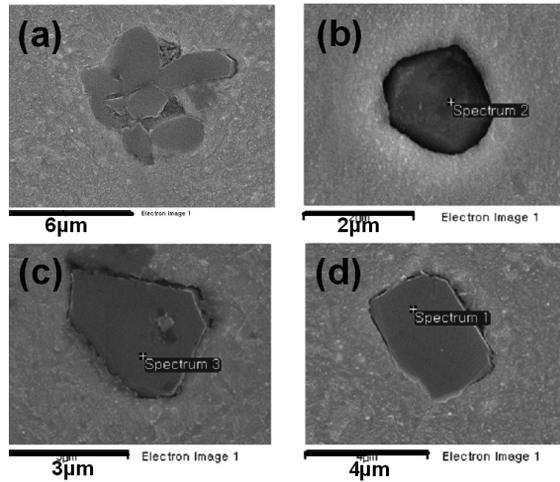after chemical reaction with Al-deoxidized molten steel

Figure 3: Typical non-metallic inclusions observed in the molten steel after reaction with the glazed refractory. (a) Al_2O_3 aggromeration – 0.5 minute, (b) spinel–0.5 minute, (c) Al_2O_3 –5 minute, and (d) spinel–15 minute

The EPMA mapping images of the glazed refractories are shown in Figure 4. Like the case for Al-deoxidized steel, the distributions of Ca and Si can give the clue for the reaction mechanism of the glazed refractory with AlCa-steel. From the Ca image, it is found that the penetration rate and depth of glaze into porous matrix are similar to the case of Al-steel. However, the Si mapping results are somewhat different. First of all, the SiO_2 concentration on the surface of the glazed refractory became diluted much faster than

for the case of the Al-steel. Almost no SiO_2 was observed on the surface after 3 minutes reacting with AlCa-steel rather than after 10 minutes reacting with Al-steel. The concentration of SiO_2 of inner side of refractory seems lower as well. The SEM images of typical inclusions are presented in Figure 5. It should be noted that the most of the non-metallic inclusions observed had spherical shapes, which means they were mostly liquid inclusions (or the mixture of liquid and solid) in experimental conditions. On the contrary, the inclusions observed with Al-steel had mostly irregular shape, which means they were in solid state in the experimental conditions. In addition, most of inclusions belonged to the CaO-MgO-Al_2O_3-CaS system. No SiO_2 element was detected in the inclusions.
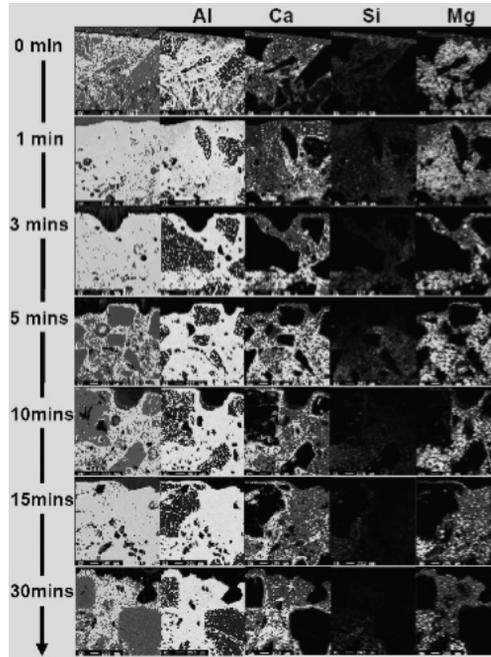

Figure 4: EPMA mapping images of the glazed refractories after chemical reaction with Al-deoxidized and Ca-treated molten steel
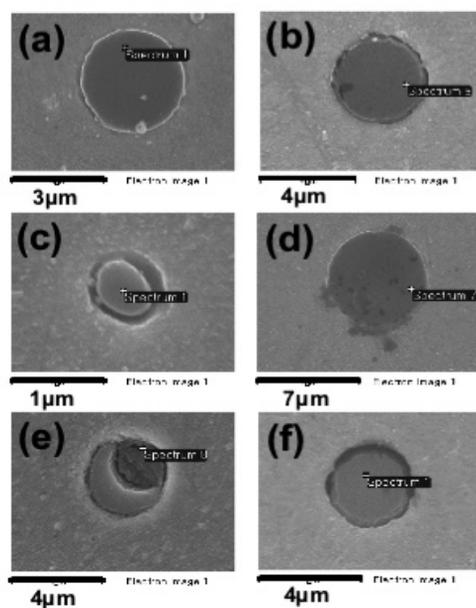
Figure 5: Typical non-metallic inclusions observed in the molten steel after reaction with the glazed refractory. (a) liquid Ca-Mg-Al-O – 0.5 minute, (b) spinel + liquid -Mg-Al-O – 0.5 minute, (c) CaS – 1 minute, (d) MgO + liquid Ca-Mg-Al-O – 1 minute, (e) CaS + Ca-Mg-Al-O-S – 15 minute, and (f) Ca-Mg-Al-O – 30 minute.

The chemistry of major inclusions in the present study were: Liquid (Ca-Al-Mg-O-S), (Liquid + solid CaS), (Liquid + solid MgO), and (Liquid + solid MgO and Spinel). The amount of CaS in liquid phase was normally less than 5 wt% except about 15 wt% CaS for (Liquid + solid CaS) inclusions. Solid Ca-Al-O inclusions ($CaAl_{12}O_{19}$, $CaAl_4O_7$ and $CaAl_2O_4$) and CaO inclusion were also observed. In the AlCa-steel sample at 30 minutes, the most of the inclusions were liquid Ca-Al-Mg-O inclusions with less than 0.5 wt% CaS.

Slag/Inclusions Interactions

As seen in the last section, the chemical interaction of ladle refractories (glaze) with the steel, in particular with Al-deoxidized steel, the eventual form of inclusions generated is mostly spinel of Al-Mg-O type. In this regard, dissolution behavior of both MgO and $MgAl_2O_4$ oxides into the $CaO-Al_2O_3-SiO_2-MgO$ slag system was studied. The slag compositions for the present study are given in Table 1.

Dissolution of MgO particles into the slag of different compositions was examined using CSLM, and the results are given in Figure 6. It is noted that the dissolution manner is vastly different for different slag compositions and prevailing temperatures. The figure shows the indirect dissolution pattern in which MgO first transforms to an intermediate reaction product which in turn dissolves into the slag. In the case of slag A at 1550ºC, $MgAl_2O_4$ spinel particles (confirmed by EPMA) formed randomly and discontinuously around the MgO particle which is transparent. In the case of slag A at 1500ºC, the MgO particle apparently lost its transparency gradually from the rim of the particle. The ring-like layer surrounding the MgO particle was found to be the intermediate product of $MgAl_2O_4$. This layer maintained its shape and position until the MgO particle completely disappeared. In the case of slag D the MgO particle lost its transparency immediately after starting dissolution presumably due to the formation of a thick layer of $MgAl_2O_4$

around the MgO particle. This dissolution pattern was the case for all three different temperatures (1550, 1500 and 1450ºC). When this happened, the rate of dissolution was much slower than other cases.
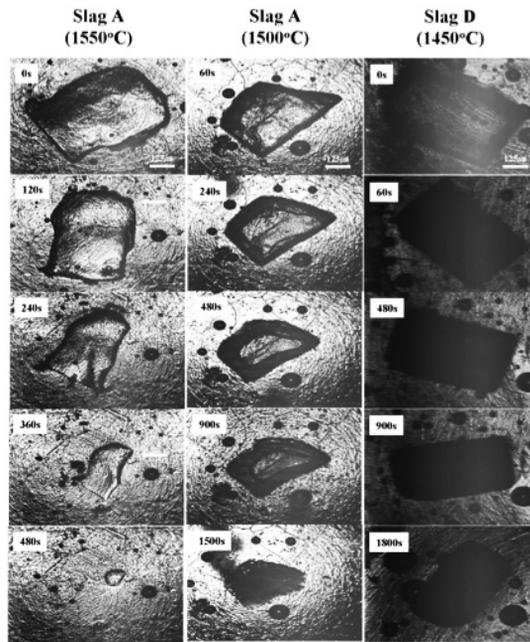

Figure 6: Dissolution of MgO particles in slag (CSLM images)

In order to investigate the dissolution patterns more closely, the samples after CSLM experiments were quenched and anayzed by the EPMA technque, and the results are shown in Figure 7. It is evident that there are three distinct patterns of the formation of intermediate products; (1) random and discontinuous pattern, (2) thin continuous pattern, and (3) thick continuous pattern. It is seen that the pattern depended both on the slag composition and temperature. For instance, at the temperature of 1500ºC a continuous layer formed for all three slags (A, C and D), but the thickness was vastly different as seen in the figure. For the same slag system A, the layer was continuous at 1500ºC, but became discontinuous at 1550ºC.
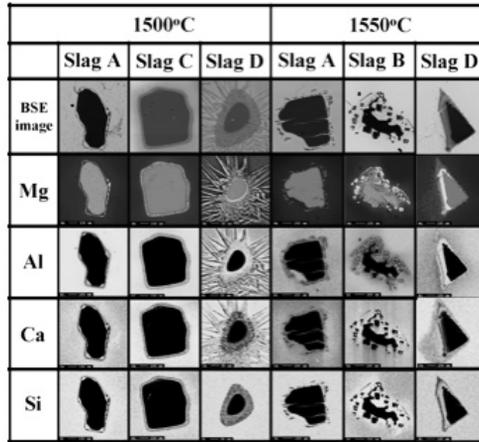
	1500°C			1550°C		
	Slag A	Slag C	Slag D	Slag A	Slag B	Slag D
BSE image						
Mg						
Al						
Ca						
Si						

Figure 7: EPMA images of indirect dissolution of MgO
particle in various CaO-Al$_2$O$_3$-SiO$_2$-MgO slags

CONCLUSIONS

Chemical interactions between Al- and Al/Ca-deoxidized steel and a high alumina refractory glazed by the typical ladle slag of CaO-MgO-Al$_2$O$_3$-SiO$_2$ was investigated to identify the influence of the glazed refractory on the generation of non-metallic inclusions. And dissolution of MgO and MgAl$_2$O$_4$ spinel particles into CaO-MgO-Al$_2$O$_3$-SiO$_2$ slag was also investigated.

The glaze layer consisted of liquid oxide phase and small amount of spinel particles. By the chemical reaction between the glazed refractory and molten steel, SiO$_2$ in the glazed refractory was reduced by Al in molten steel to increase Si content. Simultaneously, the liquid glaze reacted with the refractory, and changed gradually to the liquid CaO-Al$_2$O$_3$-MgO matrix phase with spinel and CaAl$_4$O$_7$ particles. The spinel inclusions in molten steel are believed to be generated by the direct physical detachment of spinel particles of the glaze layer and the chemical reaction between the glaze and molten steel.

In the case of Al-deoxidized and Ca-treated molten steel, various inclusions of the CaO-MgO-Al$_2$O$_3$-O-CaS were observed. The major inclusions were liquid Ca-Al-Mg-O-S inclusion, and its mixtures with solid phase such as spinel, MgO or CaS. In the earlier stage of the reaction, the inclusions of CaO, sulfide (CaS), and the Ca-Al-O (CaAl$_{12}$O$_{19}$, CaAl$_4$O$_7$ and CaAl$_2$O$_4$) were also observed frequently. With the increase of the reaction time, liquid Ca-Al-Mg-O-S inclusions became dominant in the Al-deoxidized and Ca-treated molten steel.

The dissolution behavior of MgO and MgAl$_2$O$_4$ particles into CaO-Al$_2$O$_3$-SiO$_2$-MgO slag was studied to simulate dissolution of inclusions into slag by using confocal scanning laser microscopy and EPMA. The indirect dissolution of MgO in slag involved the formation of continuous or discontinuous ring structure of MgAl$_2$O$_4$ reaction product depending on the slag composition and temperature. The indirect dissolution rate of MgO involving discontinuous ring structure was almost the same as that of direct dissolution. The continuous ring structure retarded the dissolution rate of MgO significantly approaching to that of MgAl$_2$O$_4$ direct dissolution. The form of the ring structure was closely related to the extent of the Al$_2$O$_3$ deplete zone around MgAl$_2$O$_4$ particles.

REFERENCES

Beskow, K. & Sichen, D. (2004). *Ironmaking Steelmaking.* Vol. 31, p. 393. [1]

Riaz, S., Mills, K. C. & Bain, K. (2002). *Ironmaking Steelmaking.* Vol. 29, p. 107. [2]

Hassall, G. J., Bain, K. G., Jones, N. & Warman, M. O. (2002). *Ironmaking Steelmaking.* Vol. 29, p. 383. [3]

Bygden, J., DebRoy, T. & Seetharaman, S. (1994). *Ironmaking and Steelmaking.* Vol. 21, p. 318. [4]

Zhang, P. & Seetharaman, S. (1994). J. Am. Ceram. Soc., vol. 77, p. 970. [5]

Yu, X., Pomfret, R.J. & Coley, K.S. (1997). Metall. Mater. Trans. B, Vol. 28, p. 275. [6]

Taira, S., Nakashima, K. & Mori, K. (1993). Iron Steel Inst. Jpn. Int., Vol. 33, p. 116.[7]

Son, J.-H., Jung, I.-H., Jung, S.-M., Gaye, H. & Lee, H.-G. *Chemical Reaction of Glazed Refractory with Al-deoxidized Molten Steel.* To be published. [8]

Son, J.-H., Jung, I.-H., Jung, S.-M., Gaye, H. & Lee, H.-G. (to be published). *Chemical Reaction of Glazed Refractory with Al-deoxidized & Ca-treated Molten Steel.* [9]

Park, S.-C., Jung, I.-H., Jung, S.-M., Gaye, H. & Lee, H.-G. (to be published). *Dissolution of MgO & MgAl$_2$O$_4$ Particles into CaO-Al$_2$O$_3$-SiO$_2$-MgO Slags.* [10]

Park, J.-H., Jung, I.-H. & Lee, H.-G. (2006). ISIJ Int., Vol. 46, p. 1626. [11]